Acta Cryst. (1956). 9, 304

K-Surfaces and Diffuse X-ray Reflexions

BY S. C. PRASAD AND W. A. WOOSTER

Crystallographic Laboratory, Cavendish Laboratory, Cambridge, England

(*Received* 3 *August* 1955)

The diffuse X-ray scattering from a crystal varies with direction of the wave normal of the scattering wave according to a K-factor. The method of calculating and plotting the corresponding K-surface on a stereogram is described. The construction of differential K-surfaces, for the study of the variation with the elastic constants of the K-values, is also described. Examples are given of a number of K-surfaces for tungsten, lead, iron pyrites and tin. The use of K-surfaces in the interpretation of diffuse spots on X-ray photographs is described.

Introduction

The thermal diffuse X-ray scattering from a crystal varies markedly with direction. Along any line (rekha) through a given reciprocal-lattice point (relp) the directional factor is denoted $K[ABC]_{hkl}$ (Ramachandran & Wooster, 1951). The quantities A, B, C are proportional to direction cosines of the rekha, and hkl are the indices of the relp. For a cubic crystal the expression for K may be written

$$\begin{aligned} K[ABC]_{hkl} = {} & P^2(A^{-1})_{11}+Q^2(A^{-1})_{22}+R^2(A^{-1})_{33} \\ & +2PQ(A^{-1})_{12}+2PR(A^{-1})_{13}+2QR(A^{-1})_{23}\,, \end{aligned}$$

where

$$P = h/(h^2+k^2+l^2)^{\frac{1}{2}} \text{ etc.,}$$

and

$$A_{11} = c_{11}u^2+c_{66}v^2+c_{55}w^2+2c_{56}vw+2c_{15}wu+2c_{16}uv \quad \text{etc.}$$

These expressions may be simplified by inserting the particular equalities among the c_{ik}'s of a cubic crystal, and in fact the expression may be written (Jahn, 1942)

$$\begin{aligned} K[ABC]_{hkl} = {} & [h^2\{c_{44}^2+c_{44}(c_{11}-c_{44})(v^2+w^2) \\ & +(c_{11}+c_{12})(c_{11}-c_{12}-2c_{44})v^2w^2\} \\ & +k^2\{c_{44}^2+c_{44}(c_{11}-c_{44})(w^2+u^2) \\ & +(c_{11}+c_{12})(c_{11}-c_{12}-2c_{44})w^2u^2\} \\ & +l^2\{c_{44}^2+c_{44}(c_{11}-c_{44})(u^2+v^2) \\ & +(c_{11}+c_{12})(c_{11}-c_{12}-2c_{44})u^2v^2\} \\ & -2hk(c_{12}+c_{44})\{c_{44}+(c_{11}-c_{12}-2c_{44})w^2\}uv \\ & -2kl(c_{12}+c_{44})\{c_{44}+(c_{11}-c_{12}-2c_{44})u^2\}vw \\ & -2lh(c_{12}+c_{44})\{c_{44}+(c_{11}-c_{12}-2c_{44})v^2\}wu] \\ & \div(h^2+k^2+l^2)[c_{11}c_{44}^2+c_{44}(c_{11}+c_{12}) \\ & \times(c_{11}-c_{12}-2c_{44})(u^2v^2+v^2w^2+w^2u^2) \\ & +(c_{11}+2c_{12}+c_{44})(c_{11}-c_{12}-2c_{44})^2u^2v^2w^2]\,, \end{aligned}$$

where

$$(u, v, w) = (A, B, C)/(A^2+B^2+C^2)^{\frac{1}{2}}\,.$$

By inserting particular values of the elastic constants and giving A, B, C all possible values, the whole range of K-values may be covered.

A similar computation may be carried out for a non-cubic crystal. The number of numerically different non-zero elastic constants increases as the symmetry falls, and the expressions for K contain correspondingly more terms. Although h, k, l, may have any integral values, in practice very few values suffice for the study and representation of elastic properties. For cubic crystals (100) and (110) cover most requirements; for tetragonal crystals (100), (110) and (001); and for orthorhombic crystals (100), (010), and (001). Monoclinic and triclinic crystals have not so far been studied from this point of view.

The construction of a K-surface

For cubic crystals the particular values of h, k, l and the elastic constants are inserted into the Jahn–Waller formula for $K[ABC]_{hkl}$ and the evaluation is carried out for a large number of directions defined by the direction cosines (u, v, w). The values of K are written in at the corresponding points on a stereogram and finally contours of equal K-value are drawn over the whole stereogram. In Fig. 1 the K values were calculated at all points lying on the intersections of (*a*) small circles round the [001] axis (constant ϱ-value) separated by a 10° interval, and of (*b*) great circles passing through the ends of the vertical diameter (constant φ-value) also having a 10° separation from one another. In special cases intermediate values were calculated, but usually some ninety values of K were sufficient for the construction of the K-surface. The dimensions of K are cm.^{2} dyne^{-1} and are the same as those of elastic moduli. The K-contours are therefore numbered in units of 10^{-13}.

Differential K-surfaces

If two K-surfaces are calculated on the assumption of the same values for all except one of the elastic constants, the surface obtained by plotting the difference between the K-values for corresponding points on the stereogram is known as a 'differential K-surface'. Such surfaces are applied in at least two ways.

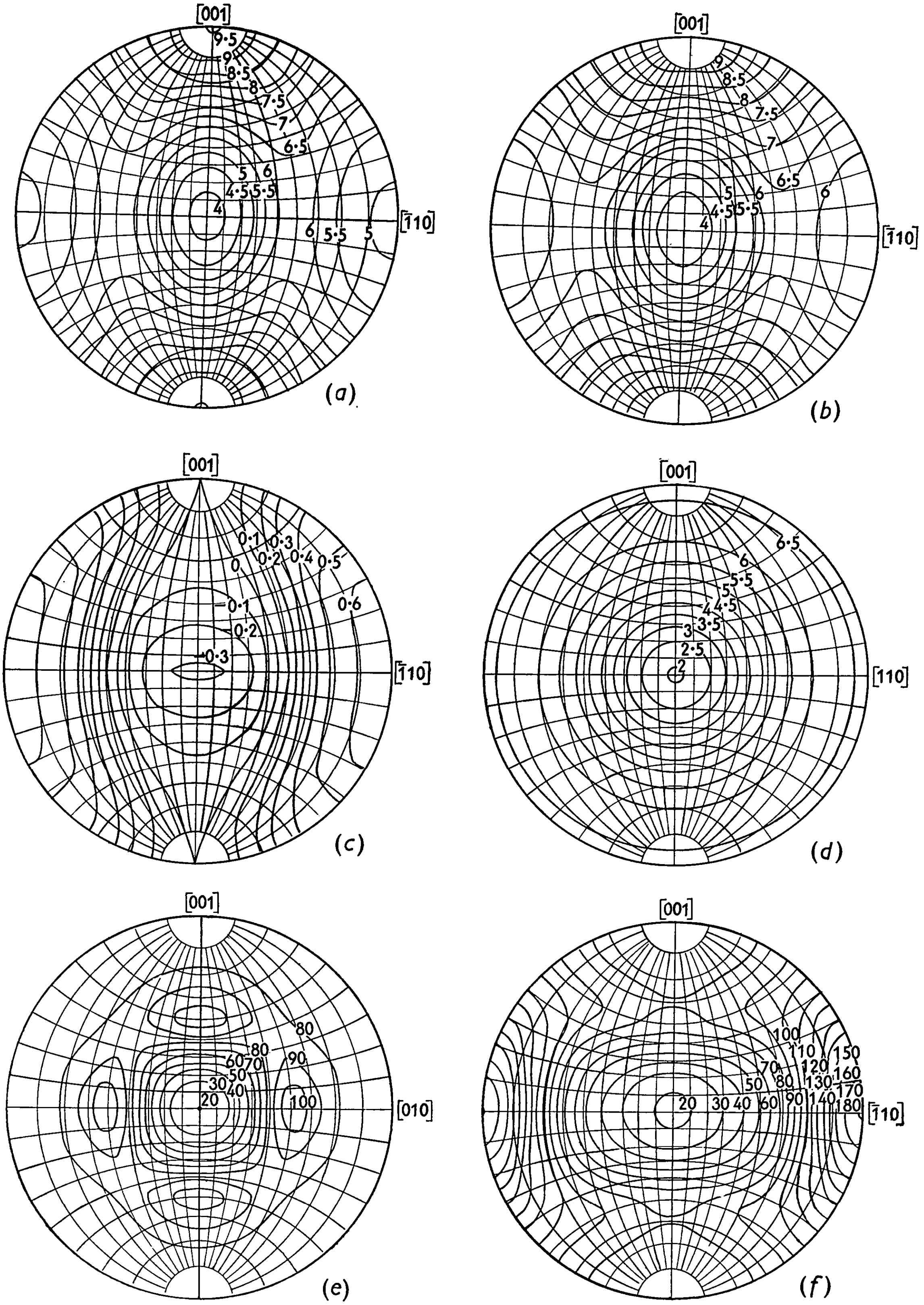
[001]
9·5
9
8·5
8
7·5
7
6·5
5
6
4·5
5·5
4
6
5·5
5
[1̄10]
(a)
[001]
9
8·5
8
7·5
7
6·5
6
5
6
4·5
5·5
4
[1̄10]
(b)
[001]
0·1
0·3
0
0·2
0·4
0·5
0·6
−0·1
−0·2
−0·3
[1̄10]
(c)
[001]
6·5
6
5·5
5
4·5
4
3·5
3
2·5
2
[110]
(d)
[001]
80
80
90
60
70
50
30
40
20
100
[010]
(e)
[001]
100
110
150
120
160
70
130
170
50
80
140
180
90
20
30
40
60
[1̄10]
(f)

Fig. 1.

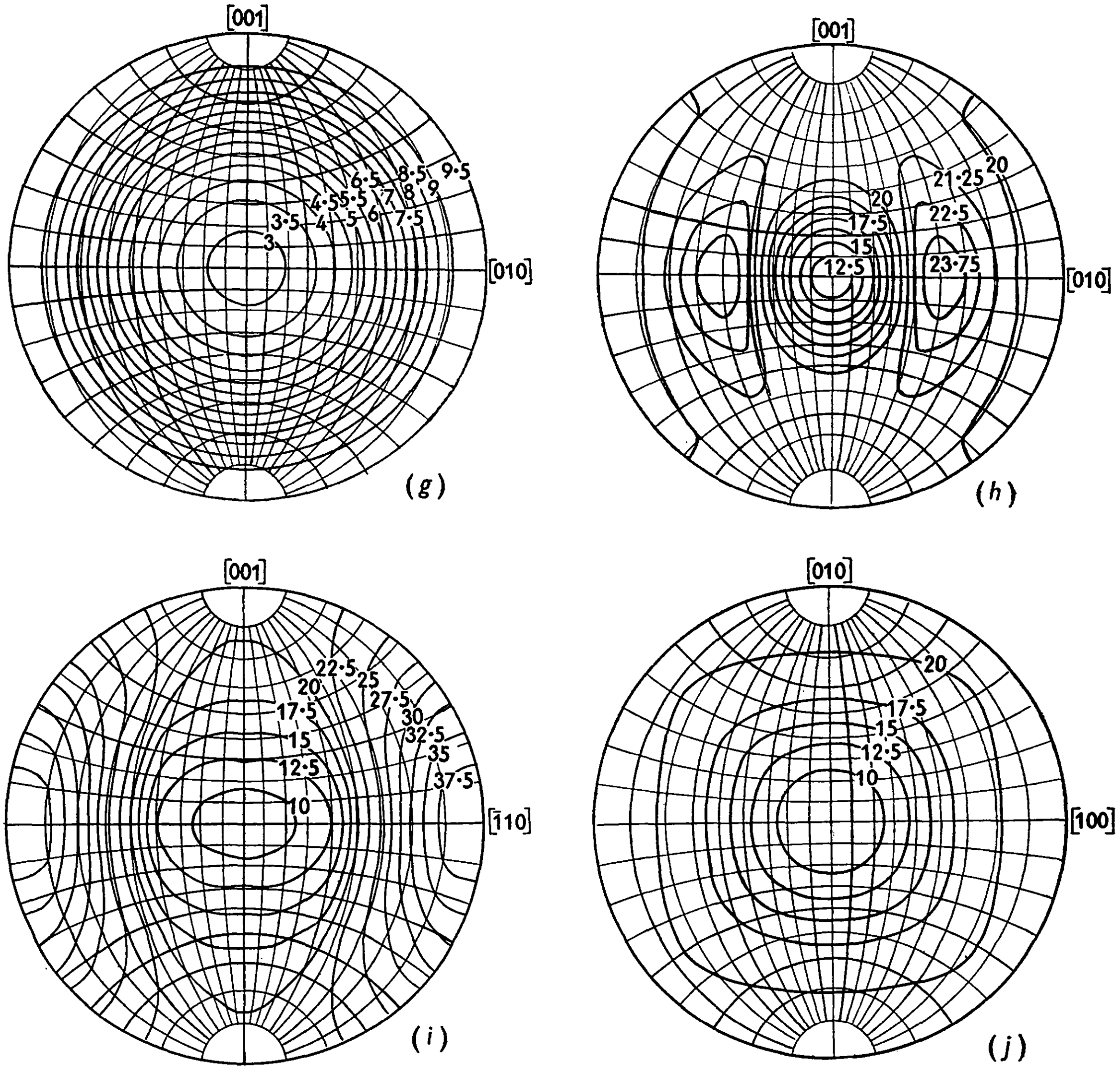

Fig. 1 (*cont.*)

Fig. 1. The stereograms represent the variation of the *K*-value with direction; the numbers against the contours are to be multiplied by 10^{-13} giving the result in cm.^{2}dyne^{-1}. (*a*) Iron pyrites, rel-vector *hh*0 (Doraiswami, 1947). (*b*) Iron pyrites, rel-vector *hh*0 (c_{11} = 36·3, c_{12} = 0·0, c_{44} = 10·5 × 10^{11} dyne cm.$^{-2}$). (*c*) Iron pyrites, rel-vector *hh*0; χ_{12} differential surface. (*d*) Tungsten, rel-vector *h*00 (Schmid & Boas, 1935). (*e*) Lead, rel-vector *h*00 (Prasad & Wooster, 1955). (*f*) Lead, rel-vector *hh*0 (Prasad & Wooster, 1955). (*g*) Iron pyrites, rel-vector *h*00 (Doraiswami, 1947). (*h*) Tin, rel-vector *h*00 (Prasad & Wooster, 1955). (*i*) Tin, rel-vector *hh*0 (Prasad & Wooster, 1955). (*j*) Tin, rel-vector 00*l* (Prasad & Wooster, 1955).

In the first application it is required to determine the *K*-surface for values of the c_{ik}'s differing slightly from those which have been used in calculating *K*-surfaces. In Fig. 1(*a*) is shown the *hh*0 *K*-surface for iron pyrites using the c_{ik}'s of Doraiswami (1947), namely $c_{11} = 36{\cdot}3$, $c_{12} = -4{\cdot}7$, $c_{44} = 10{\cdot}5 \times 10^{11}$ dyne cm.$^{-2}$ and, in Fig. 1(*b*) the corresponding *K*-surface for the values $c_{11} = 36{\cdot}3$, $c_{12} = 0{\cdot}0$, $c_{44} = 10{\cdot}5$. To obtain the *K*-surface for the Prasad & Wooster (1956*c*) set of elastic constants, which are in the same proportions as the following, namely $c_{11} = 36{\cdot}3$, $c_{12} = 3{\cdot}1$, $c_{44} = 10{\cdot}5$, the numbers on Fig. 1(*c*) were multiplied by $-3{\cdot}1/4{\cdot}7$ and new contours at intervals of 0·1 were drawn on tracing paper. This diagram was then superimposed on Fig. 1(*b*) and the *K*-values of the two figures were added and new contours were drawn corresponding to the Prasad & Wooster c_{ik}'s.

In the second application the differential *K*-surface is used to show in what sense the assumed elastic constants should be changed in order to obtain better agreement between observation and calculation. This is particularly valuable in interpreting a diffuse-reflexion photograph on which a considerable range of *K*-values is included. If at a given point on the photograph the calculated value is too small, the differential χ_{12} surface can be inspected in order to see by how much the value of χ_{12} should be changed in order to obtain agreement. The differential χ_{44} surface can also be used in the same way.

Some types of cubic *K*-surfaces

The simplest K-surfaces are shown by a crystal such as tungsten (Schmid & Boas, 1935) for which $c_{11}-c_{12}=2c_{44}$. The Jahn–Waller formula in this case becomes

$$K[uvw]_{hkl} = 1/c_{44}-(1/c_{44}-1/c_{11})(hu+kv+lw)^2/(h^2+k^2+l^2)\ .$$

For the relp 100 we have

$$K[uvw]_{100} = 1/c_{44}-(1/c_{44}-1/c_{11})u^2\ ,$$

and on the stereogram (Fig. 1(*d*)) the K-surface is represented by circles for which u is constant drawn about the rel-vector (which is at the centre of the stereogram). Since $(hu+kv+lw)$ is constant for a rekha making a given angle with the rel-vector, the formula for $K[uvw]_{hkl}$ shows that every K-surface consists of circles about the rel-vector.

The K-surfaces corresponding to $c_{11}-c_{12} < 2c_{44}$ vary considerably over the known range of values, but one example, namely that of lead, will be illustrated here. For lead $c_{11}-c_{12} = 1{\cdot}10$ and $2c_{44} = 2{\cdot}80$ (Prasad & Wooster, 1956*b*) and the 100 K-surface is shown in Fig. 1(*e*). There are pronounced peaks roughly in the direction of the diad axes. The 110 K-surface is shown in Fig. 1 (*f*) and it will be seen that is has a pronounced peak in the direction of the diad axis perpendicular to the rel-vector.

As an illustration of the case where $c_{11}-c_{12} > 2c_{44}$ the K-surfaces for iron pyrites, FeS_2, are given (Fig. 1(*a*) and (*g*)). These figures have been drawn on the assumption of the constants given by Doraiswami (1947), namely $c_{11} = 36{\cdot}3$, $c_{12} = -4{\cdot}7$, $c_{44} = 10{\cdot}5$. It is an accident that the 100 K-surface consists of circles; the 110 surface differs from the corresponding isotropic surface in not consisting of circles, described about the [001] axis.

A non-cubic *K*-surface

The 100, 110 and 001 K-surfaces of tin (Fig. 1(*h*)–(*j*)) are given as illustrations of tetragonal K-surfaces. The elastic constants used are those of Prasad & Wooster (1955), namely $c_{11} = 8{\cdot}6$, $c_{33} = 13{\cdot}3$, $c_{12} = 3{\cdot}5$, $c_{13} = 3{\cdot}0$, $c_{44} = 4{\cdot}9$, $c_{66} = 5{\cdot}3$.

The 100 surface is somewhat similar to that of lead in that in directions parallel to [110], [$\bar{1}$10] there are pronounced peaks.

The 001 surface (Fig. 1(*j*)) is plotted like all the other K-surfaces with the rel-vector at the centre of the stereogram. This implies a different relation between the angles ϱ, φ and the direction cosines u, v, w from that which applies to the 100 surface.

The use of *K*-surfaces in interpreting diffuse spots on a photograph

The diffuse spot is surveyed, using a microdensitometer, and an enlarged diagram is drawn to scale giving the experimentally observed intensity all over the spot. In dealing with the data so obtained a K-surface calculated with the appropriate elastic constants can be used in several ways.

The first application is to the divergence correction. The K-surfaces given in this paper are all appropriate to photographs which would be obtained with infinitely narrow and parallel beams of incident X-rays. The finite size of the Bragg reflexion gives a measure of the extent to which the ideal K-surface is smeared out. The K-surface is plotted so as to correspond in orientation and size with the actual photograph. For this purpose the $\bar{\varrho}$, $\bar{\varphi}$ chart (Hoerni & Wooster, 1952) is employed. The K-values are then multiplied by $(R_0/R)^2$ to correct for the various distances of the scattering points from the relp. Finally, a graphical integration over an area corresponding to the Bragg spot is made. To lessen the computational labour it is necessary to consider only certain contours along which the intensity is a given fraction of that at the centre of the diffuse spot. The effect of graphical integration is to move the contours through a greater or lesser distance from the centre. This divergence correction can be carried out on the experimentally obtained density contours but it is more convenient to use a theoretical K-surface.

In some substances, for example lead, the second-order thermal scattering is an appreciable fraction of the whole diffuse intensity and it is necessary to make allowance for this (Prasad & Wooster, 1956*b*). This can be done in a similar way to that described above for the divergence correction and can be added to the latter to obtain the total shift of the contours due to both causes.

K-surfaces are useful in showing which points on a given density contour are least likely to be affected by divergence corrections. When the contours of the K-surface are crowded together the divergence correction is less certain than when the point under study is in a region of nearly constant K-value.

Finally, K-surfaces can reveal an anomaly in the diffuse scattering due to diffuse reciprocal plates, such as occur with β-tin (Prasad & Wooster, 1956*a*). When such anomalies are present inconsistent results are obtained by taking various points from the intensity diagram. If, however, a K-surface is calculated from an assumed set of elastic constants the observed and calculated density distribution may be subtracted so as to reveal the nature of the diffuse anomaly.

One of the authors (S. C. P.) feels a great pleasure in recording his gratitude to the Government of Bihar, India, for the grant of a research scholarship and the leave for the period in which this work has been carried out.

References

DORAISWAMI, M. S. (1947). *Proc. Indian Acad. Sci.* A, **25**, 413.

HOERNI, J. A. & WOOSTER, W. A. (1952). *Acta Cryst.* **5**, 626.

JAHN, H. A. (1942). *Proc. Roy. Soc.* A, **179**, 320.

PRASAD, S. C. & WOOSTER, W. A. (1955). *Acta Cryst.* **8**, 682.

PRASAD, S. C. & WOOSTER, W. A. (1956*a*). *Acta Cryst.* **9**, 35.

PRASAD, S. C. & WOOSTER, W. A. (1956*b*). *Acta Cryst.* **9**, 38.

PRASAD, S. C. & WOOSTER, W. A. (1956*c*). *Acta Cryst.* **9**, 169.

RAMACHANDRAN, G. N. & WOOSTER, W. A. (1951). *Acta Cryst.* **4**, 335, 431.

SCHMID, E. & BOAS, W. (1935). *Kristallplastizität.* Berlin: Springer.

Acta Cryst. (1956). **9**, 308

The Crystal Structure of Rubidium Metaphosphate

BY D. E. C. CORBRIDGE

Research Department, Albright and Wilson Limited, Oldbury, Birmingham, England

(*Received* 20 *May* 1955 *and in revised form* 18 *November* 1955)

The crystal structure of rubidium metaphosphate $(RbPO_3)_n$ has been determined by three-dimensional Fourier methods. The unit cell is monoclinic with $a = 12{\cdot}123 \pm 0{\cdot}002$, $b = 4{\cdot}228 \pm 0{\cdot}002$, $c = 6{\cdot}479 \pm 0{\cdot}002$ Å, $\beta = 96° 19' \pm 20'$. The space group is $P2_1/n$ and the unit cell contains 4 units of $RbPO_3$. The structure contains continuous chains of composition $(PO_3)_n^{n-}$, which spiral round the screw axes parallel to b with a repeat pattern every two PO_3 units. These chains are held laterally by the Rb^+ ions, each of which is sevenfold co-ordinated by oxygen. Bond lengths are P–O = $1{\cdot}46 \pm 0{\cdot}03$ Å, P–O (chain) = $1{\cdot}62 \pm 0{\cdot}03$ Å. Comparisons are made with similar chain structures in metasilicates and in sulphur trioxide.

Introduction

Anions of the metaphosphate composition are known to occur in several different polymeric forms. X-ray methods have established the tetrameric ring $(PO_3)_4^{4-}$ in several crystalline salts (Pauling & Sherman, 1937; Andress, Gehring & Fischer, 1949; Romers, Ketelaar & MacGillavry, 1951) and the trimeric ring $(PO_3)_3^{3-}$ has been indicated by X-ray measurements (Cagliotti, Giacomello & Bianchi, 1942; Raistrick, 1949).

The alkali metaphosphates, in addition to forming water-soluble salts containing finite ring anions, also exist in a number of insoluble varieties. Typical of these are the 'Kurrol salts' which often appear as long fibrous crystals and which, on the basis of their colloidal and other properties, are thought to contain long chains of high molecular weight (Topley, 1949; Pfansteil & Iler, 1952; Callis, Van Wazer & Arvan, 1954). The presence of such long chains has been indicated by a brief X-ray investigation of fibrous sodium metaphosphate (Pleith & Wurster, 1951), but no complete structure determination of any compound of this type has appeared in the literature. Unit-cell and space-group data for a number of Kurrol-type salts have already been given (Corbridge, 1955). In the present work the detailed structure of one of these has been determined.

Rubidium metaphosphate was prepared by heating rubidium dihydrogen phosphate:

$$n\mathrm{RbH_2PO_4} \rightarrow (\mathrm{RbPO_3})_n + n\mathrm{H_2O}\ .$$

Small, well formed needle crystals suitable for X-ray examination were obtained by slow cooling of the metaphosphate melt.

Unit cell and space group

The unit-cell dimensions, obtained by measurement of high-angle reflexions on oscillation photographs (Farquhar & Lipson, 1946) were

$$a = 12{\cdot}123 \pm 0{\cdot}002,\ b = 4{\cdot}228 \pm 0{\cdot}002,\ c = 6{\cdot}479 \pm 0{\cdot}002\ \text{Å};\quad \beta = 96° 19' \pm 20'\ .$$

The space group was determined from zero- and first-layer Weissenberg photographs taken about the three principal axes. Observed extinctions were $\{h0l\}$ for $h+l$ odd and $\{0k0\}$ for k odd, thus giving the space group unambiguously as $P2_1/n$. The density, determined by flotation was $\varrho_o = 3{\cdot}29$ g.cm.$^{-3}$, while that calculated, assuming 4 units of $RbPO_3$ per cell, was $3{\cdot}31$ g.cm.$^{-3}$.

Experimental

Intensity data were obtained by visual estimation from Weissenberg photographs taken with Cu $K\alpha$ radiation about the three principal axes. Three films were used for each photograph which was taken twice, with a long and a short exposure, to give a set of six